

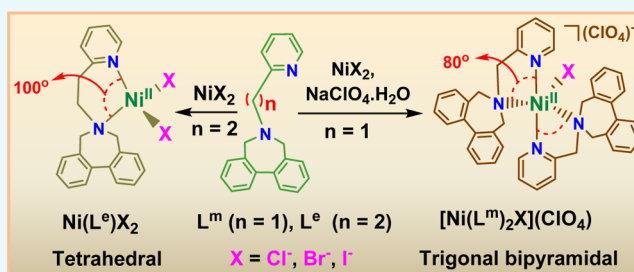
# Bite-Angle-Regulated Coordination Geometries: Tetrahedral and Trigonal Bipyramidal in Ni(II) with Biphenyl-Appended (2-Pyridyl)alkylamine *N,N'*-Bidentate Ligands

Divya Sasi, Venkatachalam Ramkumar, and Narasimha N. Murthy\*

Department of Chemistry, Indian Institute of Technology Madras, IIT Madras Campus P.O., Chennai 600036, India

**S** Supporting Information

**ABSTRACT:** Two simple biphenyl-appended (2-pyridyl)-alkylamine *N*-bidentate ligands,  $L^e$  and  $L^m$ , having ethylene and methylene spacers between donor groups, with bite angles  $L^e \approx 100^\circ$  and  $L^m \approx 80^\circ$ , dictate pseudotetrahedral and trigonal-bipyramidal geometries in six high-spin Ni(II)-halide complexes,  $[\text{Ni}(L^e)_2\text{X}_2]$  and  $[\text{Ni}(L^m)_2\text{X}](\text{ClO}_4)$  (where  $\text{X} = \text{Cl}^-, \text{Br}^-, \text{I}^-$ ), respectively. The structures in the solid state, determined using X-ray crystallography, and in solution, determined using spectroscopic methods (UV–vis–NIR and paramagnetic  $^1\text{H}$  NMR), which complement each other, are described.



## INTRODUCTION

There is growing interest directed toward the modification of classical *N*-bidentate ligands,  $\alpha$ -diimine (2,2'-bipyridine, 1,10-phenanthroline),  $\beta$ -diketiminate, diamine, and (2-pyridyl)-alkylamines to tune the steric and electronic properties to achieve novel and reactive transition metal complexes.<sup>1</sup> Low-coordinate ( $\leq 4$ ) mononuclear nickel compounds with such *N*-bidentate ligands have attracted a great deal of recent interest in the field of bioinorganic chemistry, including activation of small molecules ( $\text{O}_2$ ,  $\text{N}_2$ ,  $\text{N}_2\text{O}$ ,  $\text{NO}$ ), oxygenation catalysis, olefin polymerization, electro- and photo-catalytic hydrogen production, and other areas of applications.<sup>2–4</sup> Four-coordinate tetrahedral Ni(II)-halide complexes of sterically hindered pyridyl-imine ligands serve as alternative catalysts for traditional Ziegler–Natta polymerization of ethylene and  $\alpha$ -olefins.<sup>5</sup> Similarly, the tetrahedral Ni(II)-halide complex  $[\text{Ni}(\text{bc})\text{Cl}_2]$  ( $\text{bc} = 2,9$ -dimethyl-4,7-diphenyl-1,10-phenanthroline) functions as a photocatalyst for production of hydrogen in aqueous medium.<sup>6</sup> The classical five-coordinate Ni(II) complex,  $[\text{Ni}(\text{Me}_6\text{tren})\text{Cl}](\text{ClO}_4)$ , with magnetic anisotropy has drawn recent attention as a potential single-molecule magnet.<sup>7</sup>

Strangely, there are a limited number of four- and five-coordinate high-spin mononuclear Ni(II)-halide complexes with unhindered *N*-bidentate ligands, exhibiting tetrahedral (td) and trigonal-bipyramidal (tbp) geometries.<sup>8</sup> This is due to the plasticity of Ni(II) coordination for a range of geometries: tetrahedral, square-planar, square-pyramidal, trigonal-bipyramidal, and octahedral, which has been elegantly demonstrated recently using a chelating hemilabile P,S-bidentate ligand.<sup>9</sup> On the other hand, the use of soft donor bidentate diphosphine or hybrid P,N-ligands with methylene and ethylene spacers give low-spin square-planar Ni(II)-dichloride complexes.<sup>10</sup> Even the *N*-bidentate dihydrobis(pyrazolyl)borates with bulky substitu-

ents on the ring give square-planar and occasionally octahedral geometries.<sup>11</sup> The most common *N*-bidentate ligands, like bpy, phen, and diamine (L), typically generate tris-chelated  $[\text{NiL}_3]^{2+}$  hexacoordinate high-spin complexes,<sup>12</sup> and in solution, a dynamic equilibrium of species with different metal to ligand ratios exist.<sup>9b</sup> Even well-established versatile tridentate ligands, like triazacylononane (tacn), hydrotris(pyrazolyl)borate anion ( $\text{Tp}^-$ ), and tetradentate tris(2-pyridylmethyl)amine (tmpa), likewise give an octahedral geometry.<sup>13</sup> A few tripodal tetra-amine (tren) and tris(2-aminophenyl)amine derivatives with alkyl, aryl, amide, and urea substituents stabilize the Ni(II)-halides in the tbp geometry.<sup>7,14</sup> On the other hand, bis(imino)-pyridine and terpyridine ligands mostly give square-pyramidal geometry.<sup>15</sup> The modified bpy and phen ligands with bulky aryl/alkyl groups adjacent to *N*-donor atoms or alkylated diamines stabilize Ni(II)-dihalide in the tetrahedral geometry,<sup>16,16</sup> and less sterically hindered bidentate ligands often give halide-bridged binuclear Ni(II) complexes. However, the syntheses of such ligands with bulky substituents are sometimes challenging, either requiring expensive reagents or involving multiple steps. In addition, it has been shown that the bite angle of such rigid (bpy, phen) ligands remains unchanged ( $\sim 81^\circ$ ) and the stabilization of tetrahedral geometry is due to steric protection.<sup>1f</sup>

It is clear from the above survey that the structure and coordination geometries of Ni(II)-halide complexes are influenced by the nature of the ligand, that is, donor atom type, chelate ring size, and the steric bulk. However, control of their structures and coordination geometries by altering the bite

Received: February 2, 2017

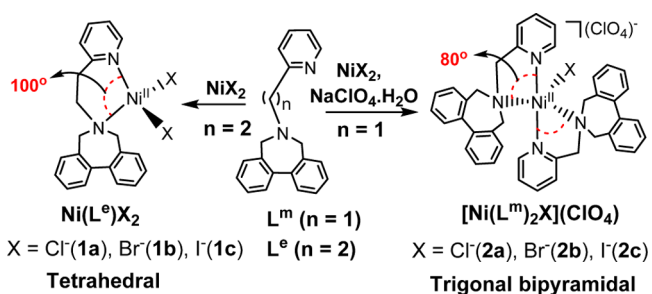
Accepted: May 17, 2017

Published: June 5, 2017

angles of bidentate ligands has not been recognized before. The vital roles of bite angles in regulating several physical and chemical properties of transition metal complexes have been documented.<sup>17</sup> The influence of wide bite angle (120°) bidentate diphosphine ligands in hydroformylation of olefins using rhodium catalyst to give stereoselective linear aldehydes has been well established, wherein they stabilize reaction intermediates in trigonal bipyramidal geometry.<sup>18</sup> Similarly, subtle changes in the bite angles of *N*-bidentate ligands influencing the spin-crossover (high-spin ↔ low-spin) transition of tris-chelated-iron complexes have been explained.<sup>17</sup>

Interestingly, the use of simple *N*-substituted (2-pyridyl)-alkylamine ligands with different alkyl spacers to stabilize different coordinate geometries of nickel(II) complexes is scarce,<sup>9,19</sup> even though they can offer a handle to alter the bite angles. We have employed two such simple biphenyl-appended (2-pyridyl)alkylamine *N,N'*-bidentate ligands having either ethyl or methyl alkyl spacers and shown how they regulate two different coordination geometries of Ni(II). The new ligands are easy to synthesize in one step and in high yields using readily available (2-pyridyl)alkylamines and 2,2'-(bromomethyl)-1,1'-biphenyl.<sup>20</sup> We have previously shown using one of the ligands ( $L^m$ , Scheme 1) with copper compounds to give unusual structures and reactivity toward dioxygen and phosphodiester substrate.<sup>21</sup>

### Scheme 1. Synthetic Route to Tetra- and Penta-Coordinate Ni(II)-Halide Complexes Dictated by the *N*-Bidentate Ligand Bite Angles



Herein, we describe the syntheses and characterization of six mononuclear high-spin Ni(II)-halide complexes,  $[\text{Ni}(L^e)\text{X}_2]$  and  $[\text{Ni}(L^m)_2\text{X}](\text{ClO}_4)$  ( $\text{X} = \text{Cl}^-, \text{Br}^-, \text{I}^-$ ), in tetrahedral and trigonal-bipyramidal geometries, regulated by the bite angles of new *N,N'*-bidentate ligands,  $L^e$  and  $L^m$ , having ethylene ( $\text{CH}_2\text{CH}_2$ ) or methylene ( $\text{CH}_2$ ) spacers between the two donor groups (Scheme 1). The work presented here represents a rare example of controlling the coordination geometries of Ni(II) by merely altering the chelate bite angles of simple *N*-bidentate ligands. The structural characterizations of all of the high-spin Ni(II) complexes in the solid state by single crystal X-ray diffraction and in solution by spectroscopic (UV–vis–NIR, ESI-MS, and paramagnetic  $^1\text{H}$  NMR) methods are described.

## RESULTS AND DISCUSSION

Treatment of the *N,N'*-bidentate ligand,  $L^e$ , with anhydrous nickel(II)-halide salts,  $\text{NiX}_2$  ( $\text{X} = \text{Cl}^-, \text{Br}^-, \text{I}^-$ ) in equimolar ratios in toluene at 50 °C for 2 h provided bluish-violet to brownish-green crystalline solids,  $[\text{Ni}(L^e)\text{X}_2]$  (where  $\text{X} = \text{Cl}^-, \text{Br}^-, \text{I}^-$ , **1a–c**) in good yield (70%). They were also prepared in tetrahydrofuran,  $\text{CH}_3\text{CN}$ , or methanol using hydrated Ni-halide salts or Ni-perchlorate in the presence of a halide source, like  $n$ -

$\text{Bu}_4\text{NX}$  or  $\text{NaX}$  ( $\text{X} = \text{Cl}, \text{Br}, \text{I}$ ). However, the yields were relatively lower because of their partial solubility in these solvents. These complexes were stable to air in the solid state and solution and soluble in chlorinated polar solvents. Efforts to prepare 1:2 Ni/ $L^e$  complexes were unsuccessful, in spite of using more than 2 equiv of ligand, clearly demonstrating the preference of ligand,  $L^e$ , for four-coordinate complexes. Contrastingly, the reaction of  $L^m$  with hydrated Ni(II)-halide salts  $\text{NiX}_2 \cdot x\text{H}_2\text{O}$  ( $\text{X} = \text{Cl}^-, \text{Br}^-, \text{I}^-$ ) in 1:2 molar ratio in methanol at room temperature, followed by the metathesis reaction with  $\text{NaClO}_4 \cdot \text{H}_2\text{O}$  readily precipitated highly crystalline apple-green to yellow-green solids,  $[\text{Ni}(L^m)_2\text{X}](\text{ClO}_4)$  ( $\text{X} = \text{Cl}^-, \text{Br}^-, \text{I}^-$ , **2a–c**) in good yield (70–75%). Like before, an attempt to prepare the 1:1 4-coordinate complex,  $[\text{Ni}(L^m)\text{Cl}_2]$  was unsuccessful, which emphasizes the preference of  $L^m$  to stabilize five-coordinate complexes.

The molecular structures of all of the six Ni(II) complexes were determined by single crystal X-ray diffraction, and as a representative example, the results of **1a** and **2a** are shown in Figure 1. The comparable structures of **1b–c** and **2b–c** are

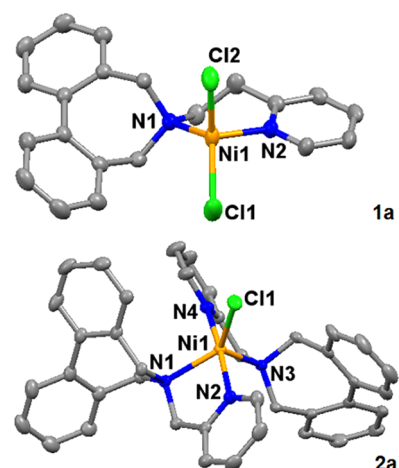


**Figure 1.** ORTEP (40% ellipsoid) plots of **1a** and  $[\mathbf{2a}]^+$ . All H-atoms and counterions are omitted for clarity.

shown in Figure S1, with selected bond lengths and angles listed in Table 1. The molecules **1a–c** are neutral four-coordinate mononuclear Ni(II) with pseudo-tetrahedral geometry, and the metal is chelated by the *N*-bidentate ligand,  $L^e$ , and two terminal halide ions. The distortion in the geometry is based on the  $\tau_4$  criterion,<sup>22</sup> 0.87 for **1a–b** and 0.97 for **1c**.

Interestingly, the opening of the  $\text{X1–Ni–X2}$  angles [ $130.74(2)$ ,  $129.00(2)$ ,  $115.53(2)^\circ$ ] compared to that in a regular tetrahedron is accompanied by closing of the ligand  $\text{N–Ni–N}$  bite angles [ $100.14(6)$ ,  $100.73(8)$ ,  $97.04(12)^\circ$ ] in **1a–c**, respectively. This is not unusual as a similar pattern has been observed with related complexes containing bis-guanidine and other hindered bidentate ligands.<sup>23</sup> It is important to point out that the ligand ( $L^e$ )  $\text{N–Ni–N}$  bite angle,  $\approx 100^\circ$  (av), is much wider than that observed ( $91^\circ$ ) for complexes containing propane-diamine,<sup>17</sup> which also form a six-membered ring, chelate, like in  $L^e$ . The wide bite angle ( $>90^\circ$ ) bidentate diamines or (2-pyridyl)alkylamines are rare.<sup>24</sup> The widening of the angle in the present case is due to the combined effect of both the ethyl spacer and sterically hindered biphenyl group. A similar example is apparent from careful analysis of a recent report on the Ni(II)-bromide complex of the *N*-substituted 2-

**Table 1. Selected Bond Lengths (Å) and Bond Angles (deg) of [Ni(L<sup>e</sup>)Cl<sub>2</sub>], 1a; [Ni(L<sup>e</sup>)Br<sub>2</sub>], 1b; [Ni(L<sup>e</sup>)I<sub>2</sub>], 1c; [Ni(L<sup>m</sup>)<sub>2</sub>Cl](ClO<sub>4</sub>)·CH<sub>2</sub>Cl<sub>2</sub>, 2a; [Ni(L<sup>m</sup>)<sub>2</sub>Br](ClO<sub>4</sub>)·CH<sub>2</sub>Cl<sub>2</sub>, 2b; and [Ni(L<sup>m</sup>)<sub>2</sub>I](ClO<sub>4</sub>), 2c Complexes**

	X =	Cl (1a)	Br (1b)	I (1c)
bond lengths	Ni1–N1	2.0463(14)	2.049(2)	2.025(3)
	Ni1–N2	1.9940(15)	1.995(2)	2.001(3)
	Ni1–X1	2.2261(6)	2.3582(5)	2.5327(6)
	Ni1–X2	2.2503(6)	2.3791(5)	2.5372(6)
bond angles	N1–Ni1–N2	100.14(6)	100.73(8)	97.04(12)
	N1–Ni1–X1	110.69(4)	111.17(6)	115.06(9)
	N1–Ni1–X2	107.00(4)	108.31(6)	111.92(9)
	N2–Ni1–X1	100.57(5)	100.35(6)	110.94(9)
	N2–Ni1–X2	102.80(5)	102.67(7)	104.17(9)
	X2–Ni1–X1	130.74(2)	129.00(2)	115.53(2)
bite angle	N1–Ni1–N2	100.14(6)	100.73(8)	97.04(12)
dihedral angle ( $\phi$ )	N1–Ni1–N2/X1–Ni1–X2	88.11	88.29	88.09
	N1–Ni1–X2/N2–Ni1–X1	87.77	86.17	86.63
	N1–Ni1–X1/N2–Ni1–X2	86.15	87.67	84.73
geometry index ( $\tau_4$ )		0.84	0.85	0.92
	X =	Cl (2a)	Br (2b)	I (2c)
bond lengths	Ni1–N1	2.149(2)	2.099(2)	2.121(3)
	Ni1–N2	2.070(3)	2.045(2)	2.044(3)
	Ni1–N3	2.104(2)	2.145(2)	2.162(3)
	Ni1–N4	2.051(3)	2.066(2)	2.047(3)
	Ni1–X1	2.3017(8)	2.4481(5)	2.6638(6)
bond angles	N1–Ni1–N2	79.17(9)	80.11(9)	80.56(12)
	N1–Ni1–N3	111.44(9)	112.17(9)	110.63(11)
	N1–Ni1–N4	94.99(10)	96.72(9)	94.81(12)
	N1–Ni1–X1	126.61(7)	121.66(7)	124.88(8)
	N2–Ni1–N3	97.01(10)	95.12(9)	94.03(12)
	N2–Ni1–N4	171.97(10)	172.21(10)	170.55(13)
	N2–Ni1–X1	94.04(7)	93.49(7)	95.21(9)
	N3–Ni1–N4	79.90(10)	79.41(9)	79.84(12)
	N3–Ni1–X1	121.95(7)	126.17(7)	124.49(8)
	N4–Ni1–X1	93.87(8)	94.22(7)	94.17(9)
bite angles	N1–Ni1–N2/N3–Ni1–N4	79.17(9)/79.90(10)	80.08(13)/79.41(9)	80.56(12)/79.84(12)
dihedral angle,	N2–C16–C17–C18–C19–C20/			
py/py ( $\phi$ )	N4–C36–C37–C38–C39–C40	75.12	76.85	77.42
geometry index ( $\tau_5$ )		0.75	0.77	0.76

(2-pyridyl)ethylamine bidentate ligand having a hindered diethyl group, which offers a wide bite angle (97°) and stabilizes the four-coordinate tetrahedral geometry.<sup>25</sup>

The Ni–N<sub>am</sub> bond is longer than Ni–N<sub>py</sub> as expected; this is due to the bulky biphenyl group on the amine nitrogen, which makes N<sub>am</sub> a weaker  $\sigma$ -donor. The coordination geometry and bond parameters of Ni(II) in 1a–c are comparable to those of related structures.<sup>6,16b,23</sup> Furthermore, the molecules in the crystal lattice are stabilized by several strong noncovalent intermolecular interactions (Figure S2, Table S2), such as hydrogen bonding (C–H...Cl, 2.85 Å, 150.8°),  $\pi$ – $\pi$  stacking (3.2 Å, py...py, face-to-face, interplanar; 3.17 Å, py...ph, face-to-side, tilted 24°), and C–H... $\pi$  (2.74 Å, CH<sub>2</sub>...ph, 141°) giving them extra stability.

On the other hand, the five-coordinate Ni(II) complexes, 2a–c, adopt a distorted trigonal-bipyramidal geometry (Figure 1, 2a), ligated by two ligand molecules, L<sup>m</sup>, providing tetra-N coordination plus a chloride (halide) ion completes the pentacoordination. The equatorial plane is made of two tertiary amine-nitrogen atoms having a bulky biphenyl append and a chloride (halide) ion. The axial positions are occupied by the nitrogen atoms of two pyridyl rings, which are nearly

orthogonal, with dihedral angles ( $\phi$ ) varying between 75.1 and 77.40° for 2a–c (Table 1). The metal atom sits almost in the trigonal plane of N<sub>1</sub>N<sub>3</sub>Cl<sub>1</sub> atoms, and the sum of the trigonal angles is 360°. However, the geometry about the metal is distorted because of the acute ligand N–Ni–N bite angles (~80° av) and hence the axial and equatorial angles deviate from the ideal, 180 and 120°, by 9°. According to the  $\tau_5$  (0.76) criterion,<sup>26</sup> the pentagonal coordination for Ni(II) is identified as distorted tpb. The geometry and coordination bond parameters of 2a–c are comparable to those of other related Ni(II) complexes containing tripodal tetra-amine-derivatives.<sup>7,14</sup> A similar example of 5-coordinate Ni(II) with tpb geometry has been recently reported with the N-substituted (2-pyridyl)methylamine ligand having a bulky (2,6-dimethyl)phenyl group.<sup>24b</sup> It re-emphasizes the role of biphenyl append in the stabilization of such an uncommon tpb geometry with Ni(II). Furthermore, strong intermolecular hydrogen bonding and  $\pi$ – $\pi$  stacking interactions, like those in 1a–c, are also observed (Figure S3).

The structures of 1a–c and 2a–c in solution, characterized by spectroscopic (UV–vis–NIR, <sup>1</sup>H NMR, ESI-MS) methods and magnetic susceptibility measurements in solution (CD<sub>2</sub>Cl<sub>2</sub>

or  $\text{CDCl}_3$ ) by Evans NMR method,<sup>27</sup> agree well with the structures observed in the solid state. The moments of **1a–c** in solution with  $\mu_{\text{eff}} \sim 3.15$  B.M. are consistent with those of Ni(II) ( $S = 1$ ) in tetrahedral geometry. Also, the moment of solid **1c** (Figure S4), with a  $\chi_{\text{M}}T$  value of  $1.1 \text{ emu mol}^{-1} \text{ K}$  ( $\mu_{\text{eff}} = 3.0$  B.M.) at 298 K, agrees with that measured in solution. The moment values,  $\mu_{\text{eff}}$  3.11, 3.47, and 3.28 B.M. for **2a–c**, respectively, are slightly greater than the spin-only value due to the spin–orbit coupling contribution. The ESI-MS spectra of complexes **2a–c** show molecular-ion peaks at  $m/z$ , 667, 711, and 757, respectively, corresponding to  $[\text{M} - \text{ClO}_4]^+$ , and the observed and calculated isotopic patterns are consistent with the expected composition (Figure S5).

The electronic absorption spectra of Ni(II) complexes in solution are characteristic of their distorted-tetrahedral and *tbp* geometries. The spectra of **1a–c** and **2a–c** were measured in  $\text{CH}_2\text{Cl}_2$ , and as a representative example, the spectra of  $[\text{Ni}(\text{L}^e)\text{Br}_2]$ , **1b**, and  $[\text{Ni}(\text{L}^m)_2\text{Br}](\text{ClO}_4)$ , **2b** are shown in Figure 2, and the comparable spectra of the remaining

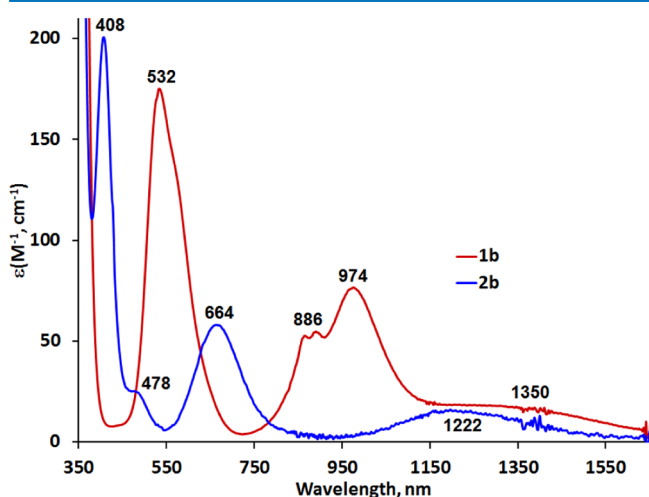


Figure 2. Electronic absorption spectra of **1b** and **2b** in  $\text{CH}_2\text{Cl}_2$ .

complexes are shown in Figure S6. The spectrum of **1b** exhibits five bands in the visible–NIR region. Both the profile and features are typical of Ni(II) in a pseudotetrahedral geometry and comparable to those of  $[\text{Ni}(\text{Tp}^{\text{Me}_2})(\text{Br})]$  (where  $\text{Tp}^{\text{Me}_2} = \text{hydrotris}(3,5\text{-dimethylpyrazole})\text{borate}$ ) having a similar geometry.<sup>28</sup> The spectrum of **1c** with two iodides is slightly different in the visible region due to a slight deviation in the coordination geometry. The spectra of complexes with *tbp* geometry **2b** (Figure 2, **2b**) and **2a,c** (Figure S7) show three well-defined bands and a shoulder at 470 nm; besides, charge transfer bands are also observed for **2b–c** in the UV-region. These features are characteristic of Ni(II)-halide complexes in the *tbp* geometry and compare well with other complexes containing tripodal tetra-amine ligands.<sup>29</sup> Furthermore, the relative shift in the absorption wavelength position among **1a–c** and **2a–c** is in accordance with the spectrochemical series  $\text{Cl} < \text{Br} < \text{I}$ .

The geometries of Ni(II) complexes in solution were easily identified by proton NMR spectroscopy.<sup>30</sup> Their paramagnetic spectra differ significantly from the corresponding diamagnetic molecules. The spectra of six-coordinate Ni(II) compounds are normally broader, whereas those for tetrahedral and trigonal-bipyramidal complexes are sharper and shifted over a wide spectral window.<sup>13c,31</sup> The  $^1\text{H}$  NMR spectra of all six complexes, **1a–c** and **2a–c**, were either measured in  $\text{CD}_2\text{Cl}_2$  or  $\text{CDCl}_3$ . As a representative example, the spectra of **1b** and **2b** are shown in Figure 3, and the rest are shown in Figures S8 and S9. The spectrum of **1b** possesses seven hyperfine-shifted resonances due to the ligand ( $\text{L}^e$ ) protons: one upfield shifted ( $-26.6$  ppm), five downfield, and a broad signal in the diamagnetic region. We assume that the isotropic shifts in all of the resonances are dominated by Fermi-contact ( $\sigma$ -delocalization), and the pseudocontact contribution is negligible. Signals were assigned on the basis of chemical shifts, integral ratio, peak widths ( $\nu_{1/2}$ ), proximity of protons to the metal center ( $\text{Ni}\cdots\text{H}$  distances from the X-ray structure of **1b**), and comparison with related examples from the literature.<sup>32</sup> The resonance at  $-26.6$  ppm is assigned to the methylene pair bound to the pyridine ring (H2), as it is common to observe this pair in the upfield region.<sup>33</sup> The other methylene pair (H1) appears at 194 ppm,

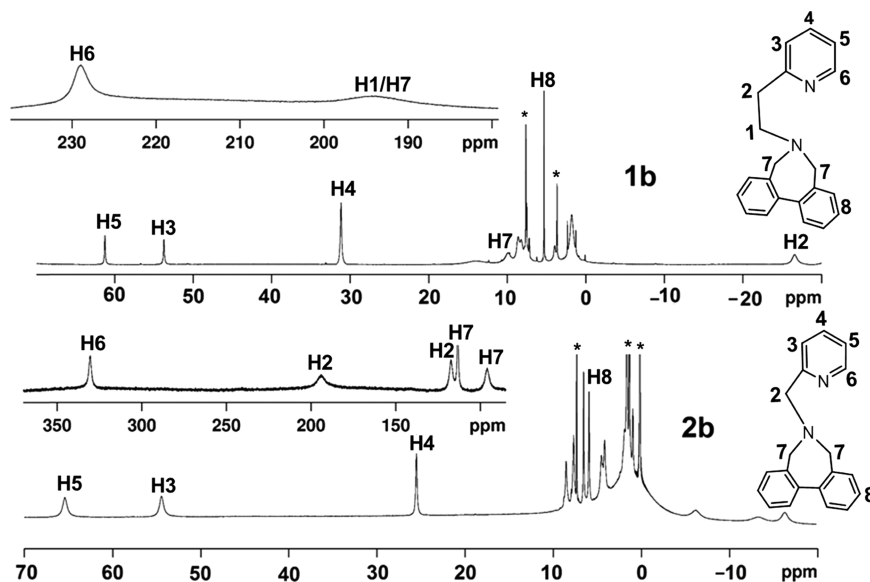


Figure 3. 500 MHz  $^1\text{H}$  NMR spectra of **1b** in  $\text{CD}_2\text{Cl}_2$  and **2b** in  $\text{CDCl}_3$ . \*Peaks due to solvent impurities.

and the two methylene pairs attached to the biphenyl ring (H7) may also have overlapped with it.<sup>34</sup> The remaining sharp signals at 228, 61, 53, and 31 ppm are typical of pyridine ring protons and assigned to H6, H5, H3, and H4, respectively. The biphenyl protons (H8) appear in the diamagnetic region, as they are too far away from the paramagnetic Ni(II) center. The spectra for the chloro and iodo derivatives, **1a** and **1c**, show a slight variation, but otherwise, the pattern remains the same. The spectral features of these complexes are comparable to those of other related tetrahedral Ni(II) complexes containing pyridine-type ligands.<sup>32</sup> On the other hand, the spectrum of **2b**, with a *tpb* geometry, shows higher contact shifts (+341 to −14 ppm) as a result of larger magnetic anisotropy due to the small bite angle of two chelated ligand molecules (*L<sup>m</sup>*).<sup>31b</sup> The two pyridine rings are equivalent, whereas the methylene groups are not. A few signals in the upfield region indicate a smaller magnetic anisotropy or a slight contribution of the pseudocontact shift. Assignment of pyridine signals was made as before; however, those due to methylene were uncertain. The NMR features can be compared with other related examples.<sup>15,35</sup>

## CONCLUSIONS

In summary, we have reported the syntheses of six new high-spin Ni(II)-halide complexes in tetrahedral and trigonal-bipyramidal geometries, regulated by the bite angles of two simple biphenyl-appended (2-pyridyl)alkylamine *N,N'*-bidentate ligands having ethylene and methylene spacers. All of the complexes, **1a–c** and **2a–c**, were characterized by single-crystal X-ray diffraction. The electronic absorption and paramagnetic proton NMR spectra in solution complemented the solid-state structures. These findings demonstrate the potential of this and related systems<sup>21</sup> to affect the metal coordination geometry and reactivity through simple ligand modifications. These complexes may have potential applications in the polymerization of olefins, similar to Brookhart catalysts,<sup>5</sup> and could even stabilize Ni(I) with phosphines as coligands and provide a pathway for hydride complexes, which may function as organometallic catalysts for hydrogenation reactions.<sup>36</sup>

## EXPERIMENTAL SECTION

All reactants were of reagent grade and used without further purification unless stated otherwise. Solvents were of HPLC quality and were freshly distilled under nitrogen before use. Dichloromethane was distilled by a standard procedure and, further, from calcium hydride. Toluene was distilled over sodium. Ethanol was purchased from Hayman and used as received. Electronic absorption spectra were recorded either on Shimadzu UV–vis 3100 or Jasco 650 spectrophotometers, and IR spectra were recorded on a Jasco 650 using the KBr pellet method. Proton nuclear magnetic resonance (<sup>1</sup>H NMR) spectra were recorded using Bruker Avance 400 and 500 spectrometers, and ESI-MS spectra were obtained in acetonitrile on a Q-TOF-Mass microhybrid quadrupole time-of-flight mass spectrometer. The vibrating sample magnetometer measurements were carried out on a Lakeshore, model 7407, with a maximum magnetic field value of 2.5 T.

**Synthesis of Metal Complexes.** Warning! Perchlorate salts are potentially explosive and should be handled only in small quantities and with care.<sup>37</sup>

The ligands, *L<sup>m</sup>* and *L<sup>e</sup>*, were prepared according to reported procedures.<sup>20</sup>

**Synthesis of [Ni(*L<sup>e</sup>*)Cl<sub>2</sub>], 1a.** To a suspension of anhydrous NiCl<sub>2</sub> (23.7 mg, 0.183 mmol) in toluene (2 mL) was added a solution of *L<sup>e</sup>* (55.0 mg, 0.183 mmol) in toluene (3 mL). The reaction mixture was heated at 50 °C to give a purple precipitate, which was filtered and dried to obtain 55.0 mg (71% yield) of **1a**. Rectangular block-shaped purple crystals were obtained by slow evaporation of CH<sub>2</sub>Cl<sub>2</sub> solution at room temperature. FT-IR (KBr, cm<sup>-1</sup>): 1608 (m), 1570 (w), 1487 (m), 1453 (s), 1417 (w), 1359 (w), 1309 (w), 1197 (w), 1158 (w), 1129 (w), 1108 (w), 1064 (w), 998 (w), 965 (w), 902 (m), 838 (w), 808 (w), 787 (s), 764 (vs), 653 (w), 608 (w), 571 (w), 499 (w), 460 (w), 421 (w). CHN analysis of [Ni(*L<sup>e</sup>*)Cl<sub>2</sub>], C<sub>21</sub>H<sub>20</sub>Cl<sub>2</sub>N<sub>2</sub>Ni: C, 58.66%; H, 4.69%; N, 6.51%; Found: C, 58.94%; H, 4.88%; N, 6.76%. UV–vis (CH<sub>2</sub>Cl<sub>2</sub>) [ $\lambda_{\text{max}}$ , nm ( $\epsilon$ , M<sup>-1</sup> cm<sup>-1</sup>): 510 (103), 838 (sh, 31), 852 (sh, 34), 950 (53), 1340 (19)]. <sup>1</sup>H NMR (CDCl<sub>3</sub>, RT):  $\delta$  −28.14 (s), 10.13 (br), 30.75 (s), 54.74 (s), 60.89 (s), 126.85 (br), 225.46 (br). Magnetic moment (Evans, CDCl<sub>3</sub>, RT): 3.15  $\mu$ B/Ni(II).

**Synthesis of [Ni(*L<sup>e</sup>*)Br<sub>2</sub>], 1b.** To a suspension of anhydrous NiBr<sub>2</sub> (33.89 mg, 0.155 mmol) in toluene (1 mL), a toluene (3 mL) solution of *L<sup>e</sup>* (46.6 mg, 0.155 mmol) was added and heated for 3 h to get a blue-violet precipitate. The precipitate upon filtration and vacuum drying gave 55.5 mg (69% yield) of **2b**. The CH<sub>2</sub>Cl<sub>2</sub> solution of **1b** when subjected to slow evaporation at room temperature yielded diamond-shaped dark blue-violet crystals. FT-IR (KBr, cm<sup>-1</sup>): 1607 (s), 1569 (w), 1487 (m), 1453 (s), 1439 (s), 1417 (m), 1358 (m), 1326 (w), 1309 (w), 1261 (w), 1211 (w), 1196 (w), 1158 (w), 1108 (m), 1087 (m), 1064 (m), 1031 (w), 1008 (w), 964 (w), 900 (m), 838 (w), 807 (m), 787 (s), 765 (vs), 653 (w), 608 (w), 570 (w), 500 (w), 460 (w), 426 (w). CHN analysis of [Ni(*L<sup>e</sup>*)Br<sub>2</sub>], C<sub>21</sub>H<sub>20</sub>Br<sub>2</sub>N<sub>2</sub>Ni: C, 48.61%; H, 3.89%; N, 5.40%; Found: C, 48.84%; H, 4.14%; N, 5.22%. UV–vis (CH<sub>2</sub>Cl<sub>2</sub>) [ $\lambda_{\text{max}}$ , nm ( $\epsilon$ , M<sup>-1</sup> cm<sup>-1</sup>): 532 (175), 864 (sh, 53), 886 (sh, 55), 974 (76), 1340 (19)]. <sup>1</sup>H NMR (CD<sub>2</sub>Cl<sub>2</sub>, RT):  $\delta$  −26.59 (br), 14.03 (br), 31.30 (s), 53.77 (s), 61.30 (s), 194.0 (br), 228.95 (br). Magnetic moment (Evans, CD<sub>2</sub>Cl<sub>2</sub>, RT): 3.14  $\mu$ B/Ni(II).

**Synthesis of [Ni(*L<sup>e</sup>*)I<sub>2</sub>], 1c.** A similar procedure to that described for **1b** was employed using anhydrous NiI<sub>2</sub> (30 mg, 0.096 mmol) and *L<sup>e</sup>* (28.8 mg, 0.096 mmol). It gave 41 mg (70.6%, yield) of a greenish-brown precipitate, soluble in CH<sub>2</sub>Cl<sub>2</sub>, CHCl<sub>3</sub>, and acetone. Recrystallization from CH<sub>2</sub>Cl<sub>2</sub> yielded diamond-shaped greenish-brown crystals. FT-IR (KBr, cm<sup>-1</sup>): 1605 (m), 1487 (m), 1474 (w), 1453 (s), 1449 (m), 1439 (s), 1390 (w), 1293 (w), 1198 (w), 1156 (w), 1115 (w), 1033 (m), 958 (w), 852 (w), 763 (vs), 615 (w), 517 (w), 420 (w). CHN analysis of [Ni(*L<sup>e</sup>*)I<sub>2</sub>], C<sub>21</sub>H<sub>20</sub>I<sub>2</sub>N<sub>2</sub>Ni: C, 41.15%; H, 3.29%; N, 4.57%; Found: C, 41.47%; H, 3.55%; N, 4.26%. UV–vis (CH<sub>2</sub>Cl<sub>2</sub>) [ $\lambda_{\text{max}}$ , nm ( $\epsilon$ , M<sup>-1</sup> cm<sup>-1</sup>): 382 (3586), 460 (2288), 568 (361), 930 (89), 1012 (77), 1340 (19)]. <sup>1</sup>H NMR (CDCl<sub>3</sub>, RT):  $\delta$  −21.51 (br), 11.69 (br), 29.29 (s), 47.15 (s), 60.69 (s), 201.38 (br).

**Synthesis of [Ni(*L<sup>m</sup>*)<sub>2</sub>Cl](ClO<sub>4</sub>), 2a.** A 2 mL MeOH solution of NiCl<sub>2</sub>·6H<sub>2</sub>O (42.7 mg, 0.179 mmol) was added to a 3 mL solution of the *L<sup>m</sup>* ligand (103 mg, 0.359 mmol) in MeOH. The reaction mixture, when stirred for about half an hour at room temperature gave a greenish-brown solution. An apple-green solid precipitated instantaneously when a 0.5 mL MeOH solution of NaClO<sub>4</sub> (22.01 mg, 0.179 mmol) was added to it. The mixture was stirred overnight, and the solid was filtered, vacuum dried, and weighed out to be 100 mg (73% yield). Deep-green block-shaped crystals were obtained by recrystal-

lization from  $\text{CH}_2\text{Cl}_2$ . FT-IR (KBr,  $\text{cm}^{-1}$ ): 1609 (s), 1572 (w), 1482 (m), 1447 (s), 1400 (w), 1372 (w), 1296 (w), 1196 (w), 1098 (vs), 929 (m), 822 (m), 753 (vs), 622 (s), 504 (w), 426 (w). CHN analysis of  $[\text{Ni}(\text{L}^m)_2\text{Cl}](\text{ClO}_4)$ ,  $\text{C}_{40}\text{H}_{36}\text{Cl}_2\text{N}_4\text{NiO}_4$ : C, 62.69%; H, 4.73%; N, 7.31%; Found: C, 62.33%; H, 4.59%; N, 7.33%. UV-vis ( $\text{CH}_2\text{Cl}_2$ ) [ $\lambda_{\text{max}}$  nm ( $\epsilon$ ,  $\text{M}^{-1}\text{cm}^{-1}$ ): 404 (127), 476 (sh, 15.8), 662 (39), 1222 (13)].  $^1\text{H}$  NMR ( $\text{CDCl}_3$ , RT):  $\delta$  -16.34 (br), -2.66 (br), 25.46 (s), 54.44 (s), 65.40 (s), 96.01 (br), 113.31 (br), 117.35 (br), 193.96 (br), 330.56 (br). Magnetic moment (Evans,  $\text{CDCl}_3$ , RT): 3.11  $\mu\text{B}/\text{Ni}(\text{II})$ . ESI-MS ( $\text{CH}_3\text{CN}$ ):  $m/z$ , 667 (85%),  $[\text{M} - \text{ClO}_4]^+$ ; 287 (100%),  $[\text{L}^m - \text{H}]^+$ ; 343 (20%),  $[\text{Ni}(\text{L}^m - \text{H})]^+$ .

**Synthesis of  $[\text{Ni}(\text{L}^m)_2\text{Br}](\text{ClO}_4)$ , **2b**.** In a reaction aimed at the preparation of **2b**, a 3 mL MeOH solution of  $\text{Ni}(\text{ClO}_4)\cdot 6\text{H}_2\text{O}$  (128 mg, 0.350 mmol) was added to a solution of  $\text{L}^m$  (200 mg, 0.698 mmol) dissolved in 1 mL of MeOH. A greenish-brown solution was obtained upon stirring for half an hour, and a green solid was precipitated when a 0.5 mL MeOH solution of *n*-tetrabutyl ammonium bromide (113 mg, 0.348 mmol) was added. The solid was filtered after stirring the mixture overnight and vacuum dried to obtain a pista-green powder that weighed 215 mg (75% yield). The complex was found to be soluble in  $\text{CH}_2\text{Cl}_2$ ,  $\text{CH}_3\text{CN}$ , and acetone and was sparingly soluble in MeOH and EtOH. The pista-green powder was recrystallized from  $\text{CH}_2\text{Cl}_2$  to give dark green diamond-shaped crystals. FT-IR (KBr,  $\text{cm}^{-1}$ ): 1609 (s), 1572 (w), 1483 (m), 1447 (m), 1400 (w), 1296 (w), 1199 (w), 1092 (vs), 928 (m), 865 (w), 821 (m), 755 (vs), 622 (s), 568 (w), 504 (w), 424 (w). CHN analysis of  $[\text{Ni}(\text{L}^m)_2\text{Br}](\text{ClO}_4)\cdot 0.5\text{CH}_2\text{Cl}_2$ ,  $\text{C}_{40}\text{H}_{36}\text{ClBrN}_4\text{NiO}_4$ : C, 57.01%; H, 4.37%; N, 6.57%. Found: C, 57.21%; H, 4.45%; N, 6.54%. UV-vis ( $\text{CH}_2\text{Cl}_2$ ) [ $\lambda_{\text{max}}$  nm ( $\epsilon$ ,  $\text{M}^{-1}\text{cm}^{-1}$ ): 322 (1390), 408 (200), 478 (sh, 25), 664 (58), 1222 (15)].  $^1\text{H}$  NMR ( $\text{CDCl}_3$ , RT):  $\delta$  -14.10 (br), -4.63 (br), 24.30 (s), 52.84 (s), 65.13 (s), 94.41 (br), 116.54 (s), 125.01 (br), 187.28 (br), 341.62 (br). Magnetic moment (Evans,  $\text{CDCl}_3$ , RT): 3.47  $\mu\text{B}/\text{Ni}(\text{II})$ . ESI-MS ( $\text{CH}_3\text{CN}$ ):  $m/z$ , 711.34 (25%),  $[\text{M} - \text{ClO}_4]^+$ ; 287 (100%),  $[\text{L}^m - \text{H}]^+$ ; 343 (20%),  $[\text{Ni}(\text{L}^m - \text{H})]^+$ .

**Synthesis of  $[\text{Ni}(\text{L}^m)_2\text{I}](\text{ClO}_4)$ , **2c**.** A 2 mL MeOH solution of  $\text{Ni}(\text{ClO}_4)\cdot 6\text{H}_2\text{O}$  (191.9 mg, 0.524 mmol) was added to 1 mL MeOH solution of  $\text{L}^m$  (300 mg, 1.05 mmol) under stirring at room temperature. The solution turned greenish-brown when stirred for about half an hour. Subsequently, the addition of NaI (78.6 mg, 0.524 mmol) resulted in a yellowish-green precipitate. The reaction mixture was stirred further for 10 h, and the complex was separated by decantation and dried. The weight of the intense yellow-green powder was 315 mg (70% yield). Recrystallization from  $\text{CH}_2\text{Cl}_2$  resulted in yellowish dark green diamond-shaped crystals. FT-IR (KBr,  $\text{cm}^{-1}$ ): 1609 (s), 1572 (w), 1483 (m), 1447 (s), 1373 (m), 1092 (vs), 928 (m), 821 (m), 757 (vs), 670 (w), 623 (s), 568 (w), 426 (w). CHN analysis of  $[\text{Ni}(\text{L}^m)_2\text{I}](\text{ClO}_4)$ ,  $\text{C}_{40}\text{H}_{36}\text{ClIN}_4\text{NiO}_4$ : C, 56.01%; H, 4.23%; N, 6.53%. Found: C, 56.50%; H, 4.17%; N, 6.46%. UV-vis ( $\text{CH}_2\text{Cl}_2$ ) [ $\lambda_{\text{max}}$  nm ( $\epsilon$ ,  $\text{M}^{-1}\text{cm}^{-1}$ ): 420 (880), 670 (75), 1222 (14)].  $^1\text{H}$  NMR ( $\text{CDCl}_3$ , RT):  $\delta$  -11.17 (br), -3.32 (br), 22.50 (s), 50.85 (s), 64.87 (s), 90.62 (br), 118.78 (s), 133.17 (br), 174.72 (br), 268 (br), 350.62 (br). Magnetic moment (Evans,  $\text{CDCl}_3$ , RT): 3.28  $\mu\text{B}/\text{Ni}(\text{II})$ . ESI-MS ( $\text{CH}_3\text{CN}$ ):  $m/z$ , 675 (90%),  $[\text{L}^m_2\text{Ni}(\text{CH}_3\text{CN})]^{2+}$ ; 512 (53%),  $[\text{L}^m\text{Ni}(\text{I})-(\text{CH}_3\text{CN})]^+$ ; 471 (53%),  $[\text{L}^m\text{Ni}(\text{I})]^+$ ; 287 (100%),  $[\text{L}^m - \text{H}]^+$ .

**Single Crystal X-ray Diffraction.** Suitable single crystals of all six compounds were mounted on thin glass fibers with epoxy glue and optically aligned on a Bruker APEX II charge-coupled device X-ray diffractometer using a digital camera. Intensity

data were measured at 25 °C using Mo  $K\alpha$  radiation ( $\lambda = 0.7103 \text{ \AA}$ ). APEX II software (Bruker AXS) was used for preliminary determination of the cell constants and data collection control. Determination of integral intensities and global refinement were performed using SAINT+ (Bruker AXS). The reflections were corrected for Lorentz and polarization effects, and empirical absorption corrections were applied using the SADABS program. The space groups were determined from systematic absences and confirmed by the results of refinement. The structures were solved by direct methods using the SHELXL software suit (SHELXS 86) and refined by the full-matrix least squares method (on  $F^2$ ; SHELXL 97). All non-H (except some of the solvent molecules) were refined with anisotropic displacement parameters, and all H atoms of the organic ligands were placed at idealized positions and refined as riding atoms.

## ■ ASSOCIATED CONTENT

### Supporting Information

The Supporting Information is available free of charge on the ACS Publications website at DOI: 10.1021/acsomega.7b00119.

Spectral data (Figures S1–S10), crystallographic data and other tables (Tables S1–S4) (PDF)

Crystallographic information files (CCDC # 1519574–1519579) (CIF)

## ■ AUTHOR INFORMATION

### Corresponding Author

\*E-mail: nnmurthy@iitm.ac.in.

### ORCID

Narasimha N. Murthy: 0000-0002-8108-3666

### Notes

The authors declare no competing financial interest.

## ■ ACKNOWLEDGMENTS

We acknowledge IIT Madras for funding the single crystal X-ray diffractometer facility.

## ■ REFERENCES

- (1) (a) Stack, T. D. P. Complexity with Simplicity: a Steric continuum of Chelating Diamines with Copper(I) and Dioxygen. *Dalton Trans.* **2003**, 1881–1889. (b) Holland, P. L. Electronic Structure and Reactivity of Three Coordinate Iron Complexes. *Acc. Chem. Res.* **2008**, *41*, 905–914. (c) Tonzetich, Z. J.; Heroguel, F.; Do, L.; Lippard, S. J. Chemistry of Nitrosyliron Complexes Supported by a  $\beta$ -Diketiminato Ligand. *Inorg. Chem.* **2011**, *50*, 1570–1579. (d) Taki, M.; Teramae, S.; Nagatomo, S.; Tachi, Y.; Kitagawa, T.; Itoh, S.; Fukuzumi, S. Fine-Tuning of Copper(I)-Dioxygen Reactivity by 2-(2-Pyridyl)ethylamine Bidentate Ligands. *J. Am. Chem. Soc.* **2002**, *124*, 6367–6377. (e) Aboeella, N. W.; Lewis, E. A.; Reynolds, A. M.; Brennessel, W. W.; Cramer, C. J.; Tolman, W. B. Snapshots of Dioxygen Activation by Copper: The Structure of a 1:1 Cu/O<sub>2</sub> Adduct and Its Use in Syntheses of Asymmetric Bis( $\mu$ -oxo) Complexes. *J. Am. Chem. Soc.* **2002**, *124*, 10660–10661. (f) Benson, E. E.; Rheingold, A. L.; Kubiak, C. P. Synthesis and Characterization of 6,6'-(2,4,6-Triisopropylphenyl)-2,2'-bipyridine(tripbipy) and Its Complexes of the Late First Row Transition Metals. *Inorg. Chem.* **2010**, *49*, 1458–1464.
- (2) (a) Yao, S.; Driess, M. Lessons from Isolable Nickel(I) Precursor Complexes for Small Molecule Activation. *Acc. Chem. Res.* **2012**, *45*, 276–287. (b) Wiese, S.; Kapoor, P.; Williams, K. D.; Warren, T. H. Nitric Oxide Oxidatively Nitrosylates Ni(I) and Cu(I) C-Organonitroso Adducts. *J. Am. Chem. Soc.* **2009**, *131*, 18105–18111. (c) Garcia-Bosch, I.; Ribas, X.; Costas, M. Well-Defined Hetero-

metallic and Unsymmetric  $M_2O_2$  Complexes Arising from Binding and Activation of  $O_2$ . *Eur. J. Inorg. Chem.* **2012**, *2012*, 179–187. (d) Rhinehart, J. L.; Brown, L. A.; Long, B. K. A Robust Ni(II)  $\alpha$ -Diimine Catalyst for High Temperature Ethylene Polymerization. *J. Am. Chem. Soc.* **2013**, *135*, 16316–16319.

(3) (a) Corona, T.; Company, A. Spectroscopically Characterized Synthetic Mononuclear Nickel–Oxygen Species. *Chem. Eur. J.* **2016**, *22*, 13422–13429. (b) Yao, S.; Bill, E.; Milsman, C.; Wieghardt, K.; Driess, M. A “Side-on” Superoxonickel Complex  $[LNi(O_2)]$  with a Square-Planar Tetracoordinate Nickel(II) Center and Its Conversion into  $[LNi(m-OH)_2 NiL]$ . *Angew. Chem., Int. Ed.* **2008**, *47*, 7110–7113.

(4) Pfirrmann, S.; Limberg, C.; Herwig, C.; Stöber, R.; Ziemer, B. A Dinuclear Nickel(I) Dinitrogen Complex and its Reduction in Single-Electron Steps. *Angew. Chem., Int. Ed.* **2009**, *48*, 3357–3361.

(5) Johnson, L. K.; Killian, C. M.; Brookhart, M. New Pd(II)- and Ni(II)-Based Catalysts for Polymerization of Ethylene and  $\alpha$ -Olefins. *J. Am. Chem. Soc.* **1995**, *117*, 6414–6415.

(6) Powers, D. C.; Anderson, B. L.; Nocera, D. G. Two-Electron HCl to  $H_2$  Photocycle Promoted by Ni(II) Polypyridyl Halide Complexes. *J. Am. Chem. Soc.* **2013**, *135*, 18876–18883.

(7) Ruamps, R.; Maurice, R.; Batchelor, L.; Boggio-Pasqua, M.; Guillot, R.; Barra, A. L.; Liu, J.; Bendeif, E.-E.; Pillet, S.; Hill, S.; Mallah, T.; Guihéry, N. Giant Ising-Type Magnetic Anisotropy in Trigonal Bipyramidal Ni(II) Complexes: Experiment and Theory. *J. Am. Chem. Soc.* **2013**, *135*, 3017–3026.

(8) Ohtsu, H.; Tanaka, K. Equilibrium of Low- and High-Spin States of Ni(II) Complexes Controlled by the Donor Ability of the Bidentate Ligands. *Inorg. Chem.* **2004**, *43*, 3024–3030.

(9) (a) Machan, C. W.; Spokoiny, A. M.; Jones, M. R.; Sarjeant, A. A.; Stern, C. L.; Mirkin, C. A. Plasticity of the Nickel(II) Coordination Environment in Complexes with Hemilabile Phosphino Thioether Ligands. *J. Am. Chem. Soc.* **2011**, *133*, 3023–3033. (b) Griend, D. A. V.; Bediako, D. K.; DeVries, M. J.; DeJong, N. A.; Heeringa, L. P. Detailed Spectroscopic, Thermodynamic, and Kinetic Characterization of Nickel(II) Complexes with 2,2'-Bipyridine and 1,10-Phenanthroline Attained via Equilibrium-Restricted Factor Analysis. *Inorg. Chem.* **2008**, *47*, 656–662.

(10) (a) Bomfim, J. A. S.; de Souza, F. P.; Filgueiras, C. A. L.; de Sousa, A. G.; Gambardella, M. T. P. Diphosphine Complexes of Nickel: Analogies in Molecular Structures and Variety in Crystalline Arrangement. *Polyhedron* **2003**, *22*, 1567–1573. (b) Speiser, F.; Braunstein, P.; Saussine, L. New Nickel Ethylene Oligomerization Catalysts Bearing Bidentate P,N-Phosphinopyridine Ligands with Different Substituents  $\alpha$  to Phosphorus. *Organometallics* **2004**, *23*, 2625–2632. (c) Hashimoto, A.; Yamaguchi, H.; Suzuki, T.; Kashiwabara, K.; Kojima, M.; Takagi, H. D. Preparation, Crystal Structures, and Spectroscopic and Redox Properties of Nickel(II) Complexes Containing Phosphane–(Amine or Quinoline)-Type Hybrid Ligands and a Nickel(I) Complex Bearing 8-(Diphenylphosphanyl)quinolone. *Eur. J. Inorg. Chem.* **2010**, *2010*, 39–47. (d) Dong, Q.; Rose, M. J.; Wong, W.-Y.; Gray, H. B. Dual Coordination Modes of Ethylene-Linked  $NP_2$  Ligands in Cobalt(II)- and Nickel(II) Iodides. *Inorg. Chem.* **2011**, *50*, 10213–10224.

(11) (a) Rheingold, A. L.; Liable-Sands, L. M.; Golen, J. A.; Yap, G. P. A.; Trofimenko, S. The Coordination Chemistry of the Hydrotris(3-Diphenylmethylpyrazol-1-yl)borate ( $Tp^{CHPh_2}$ ) Ligand. *Dalton Trans.* **2004**, 598–604. (b) Belderrain, T. R.; Paneque, M.; Carmona, E.; Gutiérrez-Puebla, E.; Monge, M. A.; Ruiz-Valero, C. Three-Center, Two-Electron M...H–B Bonds in Complexes of Ni, Co, and Fe and the Dihydrobis(3-tert-butylpyrazolyl)borate Ligand. *Inorg. Chem.* **2002**, *41*, 425–428.

(12) Ruiz-Pérez, C.; Luis, P. A. L.; Lloret, F.; Julve, M. Dimensionally Controlled Hydrogen-Bonded Nanostructures: Synthesis, Structure, Thermal and Magnetic Behaviour of the tris-(chelated)nickel(II) complex  $[Ni(bipy)_3]Cl_2 \cdot 5 \cdot H_2O$  (bipy = 2,2'-bipyridyl). *Inorg. Chim. Acta* **2002**, *336*, 131–136.

(13) (a) Amendola, V.; Boiocchi, M.; Fabbrizzi, L.; Fusco, N.; Valeri, E. The Disproportionation of  $[Ni(tacn)]^{2+}$  in  $Ni^{2+}$  and  $[Ni(tacn)_2]^{2+}$  Crystallographically Demonstrated (tacn = 1,4,7-Triazacyclononane).

*Chem. Eur. J.* **2014**, *20*, 11994–11998. (b) Desrochers, P. J.; Corken, A. L.; Tarkka, R. M.; Besel, B. M.; Mangum, E. E.; Linz, T. N. A Simple Route to Single-Scorpionate Nickel(II) Complexes with Minimum Steric Requirements. *Inorg. Chem.* **2009**, *48*, 3535–3541. (c) Szajna, E.; Dobrowolski, P.; Fuller, A. L.; Arif, A. M.; Berreau, L. M. NMR Studies of Mononuclear Octahedral Ni(II) Complexes Supported by Tris((2-pyridyl)methyl)amine-Type Ligands. *Inorg. Chem.* **2004**, *43*, 3988–3997. (d) Balamurugan, M.; Mayilmurugan, R.; Suresh, E.; Palaniandavar, M. Nickel(II) Complexes of Tripodal 4N Ligands as Catalysts for Alkane Oxidation using m-CPBA as Oxidant: Ligand Stereoelectronic Effects on Catalysis. *Dalton Trans.* **2011**, *40*, 9413–9424.

(14) (a) Chu, L.; Hardcastle, K. I.; MMacBeth, C. E. Transition Metal Complexes Supported by a Neutral Tetraamine Ligand Containing N,N-dimethylaniline Units. *Inorg. Chem.* **2010**, *49*, 7521–7529. (b) Lau, N.; Sano, Y.; Ziller, J. W.; Borovik, A. S. Terminal  $Ni^{II}$ -OH/–OH<sub>2</sub> Complexes in Trigonal Bipyramidal Geometries Derived from  $H_2O$ . *Polyhedron* **2017**, *125*, 179–185. (c) Baidya, N.; Olmstead, M.; Mascharak, P. K. Pentacoordinated Nickel(II) Complexes with Thiolato Ligation: Synthetic Strategy, Structures, and Properties. *Inorg. Chem.* **1991**, *30*, 929–937.

(15) Deb, T.; Anderson, C. M.; Ma, H.; Petersen, J. L.; Young, V. G.; Jensen, M. P. Scorpionate Halide Complexes  $[(Tp^{Ph,Me})Ni-X]$  [ $X = Cl, Br, I$ ;  $Tp^{Ph,Me} =$  Hydrotris(3-phenyl-5-methyl-1-pyrazolyl)-borate]: Structures, Spectroscopy, and Pyrazole Adducts. *Eur. J. Inorg. Chem.* **2015**, *2015*, 458–467.

(16) (a) Yang, P.; Yang, Y.; Zhang, C.; Yang, X.-J.; Hu, H.-M.; Gao, Y.; Wu, B. Synthesis, Structure, and Catalytic Ethylene Oligomerization of Nickel(II) and Cobalt(II) Complexes with Symmetrical and Unsymmetrical 2,9-diaryl-1,10-phenanthroline Ligands. *Inorg. Chim. Acta* **2009**, *362*, 89–96. (b) Jameson, G. B.; Oswald, H. R.; Beer, H. R. Structural Phase Transitions in Dihalo(N,N'-disubstituted-diazabutadiene)nickel Complexes. Structures of Bis[dibromo(N,N'-di-tert-butyl diazabutadiene)nickel] and Dibromo(N,N'-di-tert-butyl diazabutadiene)nickel. *J. Am. Chem. Soc.* **1984**, *106*, 1669–1675.

(17) Alvarez, S. Distortion Pathways of Transition Metal Coordination Polyhedra Induced by Chelating Topology. *Chem. Rev.* **2015**, *115*, 13447–13483.

(18) Casey, C. P.; Whiteker, G. T.; Melville, M. G.; Petrovich, L. M.; Gavney, J. A., Jr.; Powell, D. R. Diphosphines with natural bite angles near  $120^\circ$  increase selectivity for *n*-aldehyde formation in rhodium-catalyzed hydroformylation. *J. Am. Chem. Soc.* **1992**, *114*, 5535–5543.

(19) Zai, S.; Gao, H.; Huang, Z.; Hu, H.; Wu, H.; Wu, Q. Substituent Effects of Pyridine-amine Nickel Catalyst Precursors on Ethylene Polymerization. *ACS Catal.* **2012**, *2*, 433–440.

(20) Sabiah, S. Bioinspired Copper Complexes for Activation of  $O_2$  and Phosphodiester: Structural, Spectroscopic, Magnetic and Reactivity Studies. Ph.D. Thesis, Indian Institute of Technology Madras, October 2007.

(21) Sabiah, S.; Varghese, B.; Murthy, N. N. First Hexanuclear Copper(II) pyrophosphate through Hydrolysis of Phosphodiester with a Dicopper Complex. *Chem. Commun.* **2009**, 5636–5638.

(22) Yang, L.; Powell, D. R.; Houser, R. P. Structural Variation in Copper(I) Complexes with Pyridylmethylamide Ligands: Structural Analysis with a New Four-coordinate Geometry index,  $\tau_4$ . *Dalton Trans.* **2007**, 955–964.

(23) Roquette, P.; König, C.; Hübner, O.; Wagner, N.; Kaifer, E.; Enders, M.; Himmel, H.-J. Mono- and Dinuclear  $Ni^{II}$  and  $Co^{II}$  Complexes that Feature Chelating Guanidine Ligands: Structural Characteristics and Molecular Magnetism. *Eur. J. Inorg. Chem.* **2010**, *2010*, 4770–4782.

(24) (a) van der Veen, L. A.; Keeven, P. K.; Kamer, P. C. J.; van Leeuwen, P. W. N. M. Wide bite angle amine, arsine and phosphine ligands in rhodium- and platinum/tin-catalysed hydroformylation. *J. Chem. Soc., Dalton Trans.* **2000**, 2105–2112. (b) Aguilà, D.; Escribano, E.; Speed, S.; Talancón, D.; Yermán, L.; Alvarez, S. Calibrating the coordination chemistry tool chest: metrics of bi- and tridentate ligands. *Dalton Trans.* **2009**, 6610–6625.

(25) Lin, Y.-C.; Yu, K.-H.; Lin, Y.-F.; Lee, G.-H.; Wang, Y.; Liu, S.-T.; Chen, J.-T. Synthesis, structures of (aminopyridine)nickel complexes and their use for catalytic ethylene polymerization. *Dalton Trans.* **2012**, *41*, 6661–6670.

(26) Addison, A. W.; Rao, T. N.; Reedijk, J.; van Rijn, J.; Verschoor, G. C. Synthesis, Structure, and Spectroscopic Properties of Copper(II) Compounds Containing Nitrogen–sulphur Donor Ligands; the Crystal and Molecular Structure of Aqua[1,7-bis(N-methylbenzimidazol-2'-yl)-2,6-dithiaheptane]copper(II) perchlorate. *J. Chem. Soc., Dalton Trans.* **1984**, 1349–1356.

(27) Evans, D. F.; Jakubovic, D. A. Water-soluble Hexadentate Schiff-base Ligands as Sequestering Agents for Iron(III) and Gallium(III). *J. Chem. Soc., Dalton Trans.* **1988**, 2927–2933.

(28) (a) Desrochers, P. J.; Telsler, J.; Zvyagin, S. A.; Ozarowski, A.; Krzystek, J.; Vivic, D. A. Electronic Structure of Four-Coordinate C<sub>3v</sub> Nickel(II) Scorpionate Complexes: Investigation by High-Frequency and -Field Electron Paramagnetic Resonance and Electronic Absorption Spectroscopies. *Inorg. Chem.* **2006**, *45*, 8930–8941. (b) Lever, A. B. P. *Inorganic Electronic Spectroscopy*, 2nd ed.; Elsevier: Amsterdam, 1986; pp 525–534.

(29) Fenton, N. D.; Gerloch, M. Energies, Intensities, and Circular Dichroism of d-d Transitions in Trigonal-Bipyramidal Cobalt(II) and Nickel(II) Chromophores. *Inorg. Chem.* **1990**, *29*, 3726–3733.

(30) Bertini, I.; Luchinat, C. *NMR of Paramagnetic Molecules in Biological Systems*; Benjamin & Cummings: Menlo Park, CA, 1986; pp 19–46.

(31) (a) Belle, C.; Bougault, C.; Averbuch, M.-T.; Durif, A.; Pierre, J.-L.; Latour, J.; Le Pape, L. Paramagnetic NMR Investigations of High-Spin Nickel(II) Complexes. Controlled Synthesis, Structural, Electronic, and Magnetic Properties of Dinuclear vs Mononuclear Species. *J. Am. Chem. Soc.* **2001**, *123*, 8053–8066. (b) Holz, R. C.; Evdokimov, E. A.; Gobena, F. T. Two-Dimensional <sup>1</sup>H NMR Studies on Octahedral Nickel(II) Complexes. *Inorg. Chem.* **1996**, *35*, 3808–3814.

(32) (a) Roquette, P.; Maronna, A.; Reinmuth, M.; Kaifer, E.; Enders, M.; Himmel, H.-J. Combining NMR of Dynamic and Paramagnetic Molecules: Fluxional High-Spin Nickel(II) Complexes Bearing Bisguanidine Ligands. *Inorg. Chem.* **2011**, *50*, 1942–1955. (b) Soshnikov, I. E.; Semikolenova, N. V.; Bryliakov, K. P.; Zakharov, V. A.; Sun, W.-H.; Talsi, E. P. NMR and EPR Spectroscopic Identification of Intermediates Formed upon Activation of 8-Mesitylimino-5,6,7-trihydroquinolynickel Dichloride with AlR<sub>2</sub>Cl (R = Me, Et). *Organometallics* **2015**, *34*, 3222–3227.

(33) (a) Murthy, N. N.; Karlin, K. D.; Bertini, I.; Luchinat, C. NMR and Electronic Relaxation in Paramagnetic Dicopper(II) Compounds. *J. Am. Chem. Soc.* **1997**, *119*, 2156–2162. (b) Karlin, K. D.; Nanthakumar, A.; Fox, S.; Murthy, N. N.; Ravi, N.; Huynh, B. H.; Orosz, D.; Day, E. P. X-ray Structure and Physical Properties of the Oxo-Bridged Complex [(F<sub>8</sub>-TPP)Fe-O-Cu(TMPA)]<sup>+</sup>, F<sub>8</sub>-TPP = Tetrakis(2,6-difluorophenyl)porphyrinate(2-), TMPA = Tris(2-pyridylmethyl)amine: Modeling the Cytochrome c Oxidase Fe-Cu Heterodinuclear Active Site. *J. Am. Chem. Soc.* **1994**, *116*, 4753–4763.

(34) La Mar, G. N.; Sacconi, L. Proton Magnetic Resonance Studies of High-Spin Nickel(II) Complexes with Pentadentate Schiff Bases. *J. Am. Chem. Soc.* **1967**, *89*, 2282–2291.

(35) (a) Jones, M. B.; Newell, B. S.; Hoffert, W. A.; Hardcastle, K. I.; Shores, M. P.; MacBeth, C. E. Chelating Tris(amidate) Ligands: Versatile Scaffolds for Nickel(II). *Dalton Trans.* **2010**, *39*, 401–410. (b) Luca, O. R.; Konezny, S. J.; Paulson, E. K.; Habib, F.; Luthy, K. M.; Murugesu, M.; Crabtree, R. H.; Batista, V. S. Study of an S = 1 Ni<sup>II</sup> Pincer Electrocatalyst Precursor for Aqueous Hydrogen Production Based on Paramagnetic <sup>1</sup>H NMR. *Dalton Trans.* **2013**, *42*, 8802–8807.

(36) Berning, D. E.; Noll, B. C.; DuBois, D. L. Relative Hydride, Proton, and Hydrogen Atom Transfer Abilities of [HM-(diphosphine)<sub>2</sub>]PF<sub>6</sub> Complexes (M = Pt, Ni). *J. Am. Chem. Soc.* **1999**, *121*, 11432–11447.

(37) Wolsey, W. C. Perchlorate Salts, Their Uses and Alternatives. *J. Chem. Educ.* **1973**, *50*, A335–A337.